Electronic Supplementary Information

Predicting and rationalizing the effect of surface charge distribution and orientation on nano-wire based FET bio-sensors

Luca De Vico, Lars Iversen, Martin H. Sørensen, Mads Brandbyge, Jesper Nygård, Karen L. Martinez, Jan H. Jensen

Contents

List of Figures

List of Tables

Conductance sensitivity with SMSCSL

The base conductance G_0 of a cylindrical nano wire can be expressed as:

$$G_0 = \frac{\pi R^2 e\,(n_0\,\mu_n + p_0\,\mu_p)}{L} \tag{S1}$$

where R is the radius of the wire, e the elementary charge, n_0 the wire electron density, μ_n the wire electron mobility, p_0 the wire hole density, μ_p the wire hole mobility and L the length of the wire. For a nano-wire material with high enough doping, Equation (S1) can be approximated by considering only the electron or the hole density (only n_0 or p_0) and mobility (indicated simply as μ). For example, for a p-type doped nano-wire, it is possible to rewrite Equation (S1) as:

$$G_0 = \frac{\pi R^2 e\,p_0\,\mu}{L} \tag{S2}$$

Following Sørensen et al. equations,[1] one can define the generic sensitivity of a cylindric nano wire as:

$$\frac{\Delta G}{G_0} = -\frac{2}{R e\,p_0}\Gamma\sigma_s \tag{S3}$$

where σ_s is the "sensed" charge density at the surface of the wire and Γ a dimensionless function quantifying the actual sensitivity of the nano-wire.
In the special case of a cylindrical nano-wire it is possible to express Γ analytically as:[2]

$$\Gamma = \frac{\varepsilon_1 K_0\left(\frac{R+\Delta R}{\lambda_D}\right)\frac{\lambda_D}{\lambda_{TF}} I_1\left(\frac{R}{\lambda_{TF}}\right)}{\left[K_0\left(\frac{R+\Delta R}{\lambda_D}\right)\left(\frac{\lambda_D}{R+\Delta R}\right) + \ln\left(\frac{R+\Delta R}{R}\right) K_1\left(\frac{R+\Delta R}{\lambda_D}\right)\frac{\varepsilon_3}{\varepsilon_2}\right]\varepsilon_1\left(\frac{R}{\lambda_{TF}}\right) I_1\left(\frac{R}{\lambda_{TF}}\right) + \varepsilon_3 K_1\left(\frac{R+\Delta R}{\lambda_D}\right) I_0\left(\frac{R}{\lambda_{TF}}\right)} \tag{S4}$$

where λ_D is the Debye length of the buffer, λ_{TF} the Thomas-Fermi distance typical of the wire material, ε_1, ε_2 and ε_3 are the relative permittivities of the wire, the oxide layer and the buffer, respectively, ΔR is the oxide layer thickness, I_0, I_1, K_0 and K_1 are the modified Bessel functions of first and second kind, respectively.[3] Equation (S4) differs from the one reported in Ref. 1 since it considers explicitly a finite thickness for the oxide layer.

When considering the presence of additional charges at a distance l from the wire that gives rise to a charge density σ_b, it is possible to rewrite Equation (S3) as:

$$\frac{\Delta G}{G_0} = -\frac{2}{R e\,p_0}\Gamma\left(\Gamma_l\,\sigma_b + \sigma_s\right) \tag{S5}$$

where Γ_l is defined as in Equation (7) of Ref. 1:

$$\Gamma_l = 2\frac{R}{R+l}\left(1+\sqrt{\frac{R}{R+l}}\exp(l/\lambda_D)\right)^{-1} \tag{S6}$$

In the multiple charges model a series of m charges Q_i with distance l_i from the nano-wire surface gives rise to σ_{b_i} charge densities. The complete expression for the sensitivity is then given by:

$$\frac{\Delta G}{G_0} = -\frac{2}{R e\,p_0}\Gamma\left[\sigma_s + \sum_i^m\left(\Gamma_{l_i}\,\sigma_{b_i}\right)\right] \tag{S7}$$

In the current contribution we assumed that the binding event does not perturb sensibly the charges already present on the surface of the nano-wire. σ_s can then be omitted, giving Equation (1). σ_{b_i} is computed as reported in Equation (2).

For a n-type nano-wire based BIOFET it is necessary to remove the factor -1 in Equations (1), (S3) and (S5), and use the appropriate value for the charge carrier density (n_0 instead of p_0) and mobility where needed.

The various parameters and their interpretation inside the multiple charges model are depicted in Fig. 1.

Buffer solution Debye length

Ions dissolved in solution lower the effectiveness of analyte charge(s) on the BIOFET signal. This effect is known as Debye screening and its characteristic Debye length λ_D can be evaluated as:

$$\lambda_D = \sqrt{\frac{\varepsilon_0 \varepsilon_3 K T}{2 N_A e^2 I}} \tag{S8}$$

$$I = \frac{1}{2} \sum_{B=1}^{n} C_B Z_B^2 \tag{S9}$$

where ε_0 is the vacuum permittivity, K is the Boltzmann constant, T is the absolute temperature of the experiment (298.15 K), N_A is the Avogadro number and I is the ionic strength of the solution, which is based on the concentration C and charge Z of each ionic species present in the buffer.

Simulated nano-wire characteristics

To evaluate the change in conductance sensitivity (signal) depending on the different charge systems, we need to define a nano-wire based BIOFET device for all our determinations. We consider a cylindric nano-wire. For p-type silicon nano-wire, we base our choice of parameters on the data reported by the Lieber group as described in Ref. 4, with the characteristics reported in Table 1S†. By using the average values[4] for the nano-wire radius, length, mobility and base transconductance, it is possible to retrieve an average value for the hole density p_0 following Equation (S10), inverse of Equation (S2):

$$p_0 = \frac{G_0 L}{\pi R^2 e \mu} \tag{S10}$$

In this way we can retrieve the average value for p_0 reported in Table 1S†. The value for the Thomas-Fermi length is computed using the following equation:

$$\lambda_{TF} = \sqrt{\frac{\hbar^2 \varepsilon_r \pi^{4/3}}{m^* e^2 p_0^{1/3}}} \tag{S11}$$

where $\varepsilon_r = \varepsilon_0 \varepsilon_1$ and the effective hole mass m^* value was set to 0.54 times the mass of an electron at rest.[5] The value for the mobility μ reported in Table 1S† differs from the value (0.056 $m^2V^{-1}s^{-1}$) reported as average in Ref. 4. In fact we decide to lower such value to 0.01 in order to simulate the effects of the chemical treatments to which the wires are subjected when transformed into BIOFETs, since found appropriate in previous studies.[6]

For n-type In_2O_3 nano-wire, we base our parameters on different sources.[7–11] Its characteristics are reported in Table 2S†. In order to apply Equation (S11) the value for m^* was set to 0.35 times the mass of an electron at rest.[10] In Equations (S10) and (S11) p_0 has to be substituted with n_0.

Charge of a ionizable amino acid

For the ionizable amino acids HIS, LYS, ARG and the N terminal, the charge at a given pH value can be expressed as:

$$q = \frac{10^{pK_a - pH}}{1 + 10^{pK_a - pH}} \tag{S12}$$

For the ionizable amino acids ASP, GLU, CYS, TYR and the C terminal the charge is computed as $q' = q - 1$.

Table 1S† Parameters defining the simulated silicon p-type doped nano-wire based BIOFET.

Parameter	Symbol	Value	(units)
Length	L	2000.0	(nm)
Radius	R	10.0	(nm)
Oxide layer thickness	ΔR	2.0	(nm)
Thomas-Fermi Length	λ_{TF}	2.04	(nm)
Charge carrier density	p_0	$1.11E^{24}$	(m^{-3})
Charge carrier mobility	μ	0.01	$(m^2V^{-1}s^{-1})$
Wire permittivity	ε_1	12.0	(ε_0)
Oxide layer permittivity	ε_2	3.9	(ε_0)
Solvent permittivity	ε_3	78.0	(ε_0)

Table 2S† Parameters defining the simulated In_2O_3 n-type semiconducting nano-wire based device, as retrieved from different sources.[7–11]

Parameter	Symbol	Value	(units)	Reference
Length	L	2000.0	(nm)	9
Radius	R	5.0	(nm)	9
Oxide layer thickness	ΔR	0.0	(nm)	11
Thomas-Fermi Length	λ_{TF}	1.179	(nm)	[a]
Charge carrier density	n_0	$4.6E^{25}$	(m^{-3})	7
Charge carrier mobility	μ	0.0078	$(m^2V^{-1}s^{-1})$	7
Wire permittivity	ε_1	9.0	(ε_0)	7,8
Solvent permittivity	ε_3	78.0	(ε_0)	

[a] Value obtained with Equation (S11) and the data from Ref. 10.

Other biomolecule mimicking charge distributions

Fig. 1S† Dependence of the conductance sensitivity (signal) of a Si p-type doped nano-BIOFET on the Debye length λ_D. Different biomolecule models are reported, each constituted by five charges ($m = 5$) at constant internal distances. The signal is evaluated at different distances D (in nm) from the nano-wire surface. a) Linear disposition, system charge -2, and b) their predicted signal. c) Compact disposition, system charge -3, and d) their predicted signal.

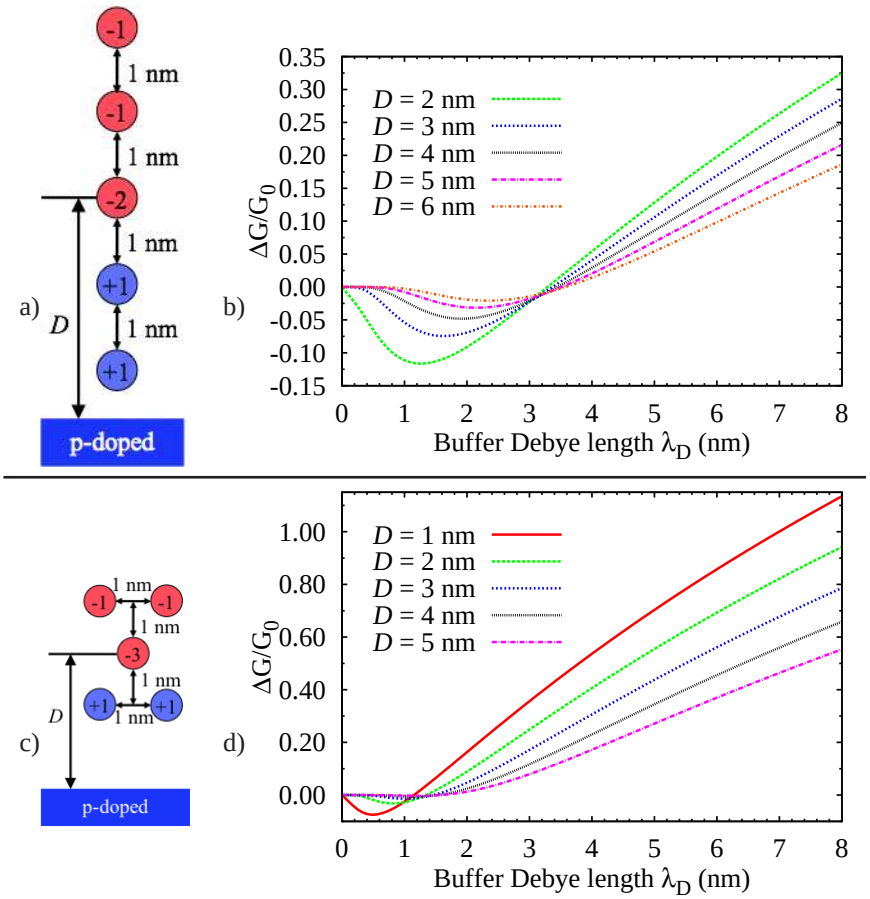

Fig. 2S† Dependence of the conductance sensitivity (signal) of a Si p-type doped nano-BIOFET on the Debye length λ_D. Different biomolecule models are reported, each constituted by three charges ($m = 3$, system charge -1) at constant internal distances, as reported. The signal is evaluated at different distances D (in nm) from the nano-wire surface. a) 0.5 nm inter-charge distance and b) the predicted signal. c) 1.0 nm inter-charge distance and d) the predicted signal with e) a detailed view of the **ZSP** region. f) 1.5 nm inter-charge distance and g) the predicted signal. The c and d panels are the same as in Fig. 2e,f.

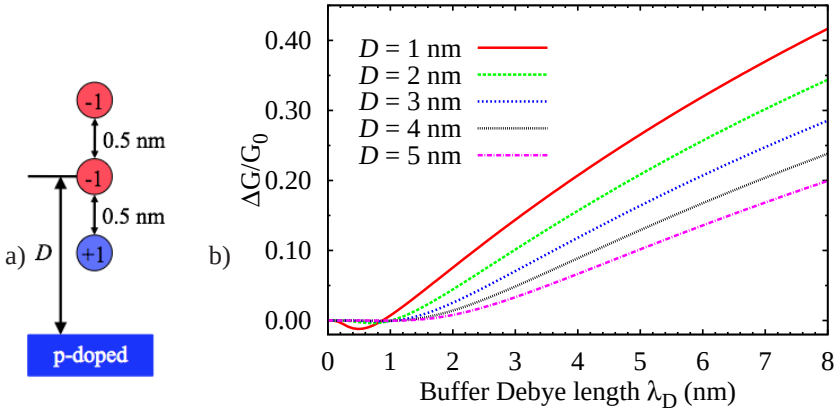

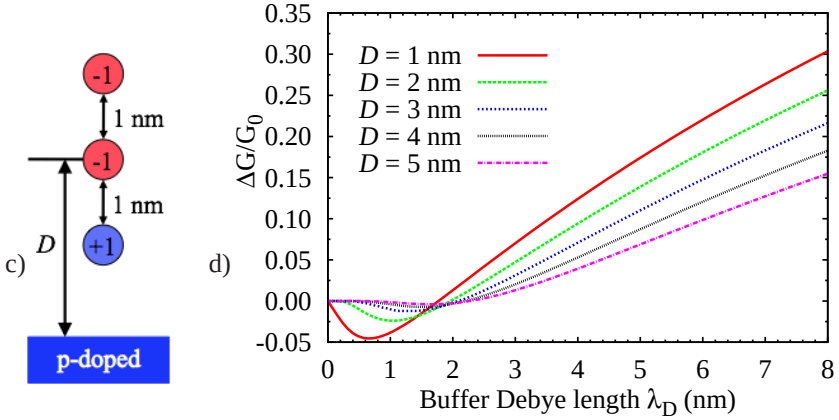

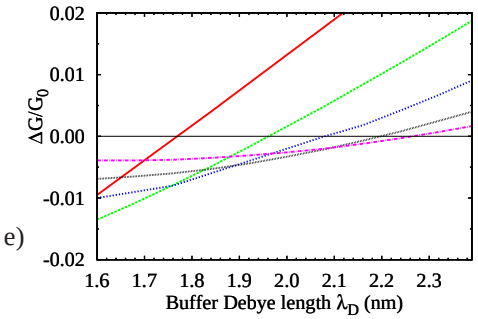

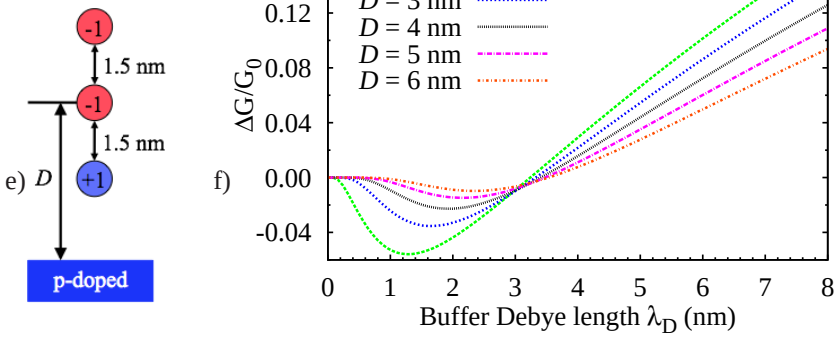

Fig. 3S† Dependence of the conductance sensitivity (signal) of a Si p-type doped nano-BIOFET on the Debye length λ_D. The reported biomolecule model is constituted by $m = 3$ charges (system charge -1) at constant internal distances. The signal is evaluated at $D = 1$ nm for different Thomas-Fermi lengths. a) The system and b) its predicted signal for different values of λ_{TF}.

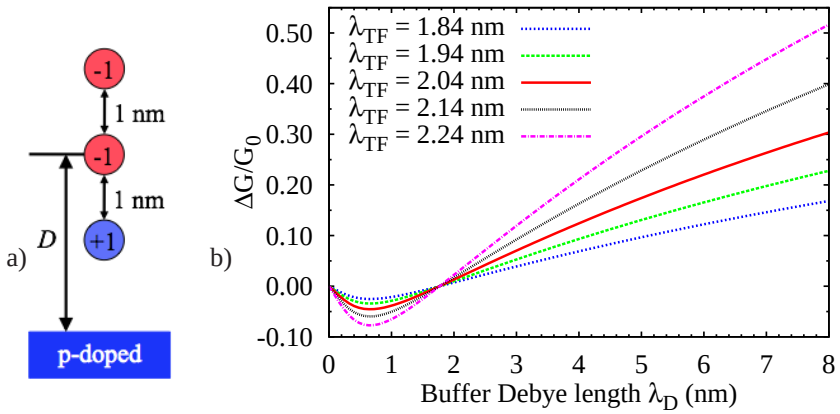

Fig. 4S† Dependence of the conductance sensitivity (signal) of a Si p-type doped nano-BIOFET on the Debye length λ_D. The reported biomolecule model is constituted by $m = 2$ charges (system charge -1) at constant internal distances. The signal is evaluated at different distances D (in nm) from the nano-wire surface. a) The system and b) its predicted signal.

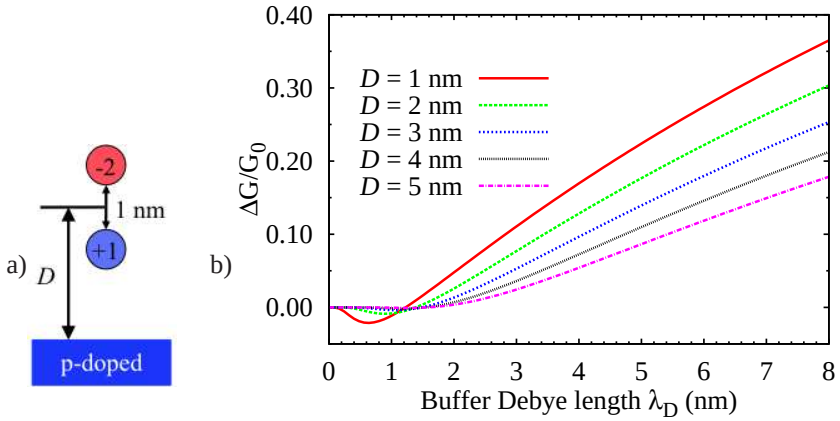

Fig. 5S† Dependence of the conductance sensitivity (signal) of a Si p-type doped nano-BIOFET on the Debye length λ_D. The reported biomolecule model is constituted by $m = 3$ charges (system charge +1) at constant internal distances. The signal is evaluated at different distances D (in nm) from the nano-wire surface. a) The system and b) its predicted signal.

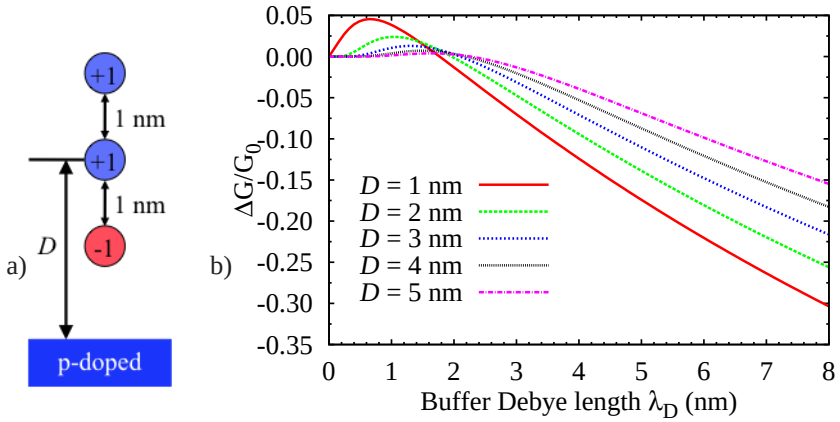

Fig. 6S† Dependence of the conductance sensitivity (signal) of a Si p-type doped nano-BIOFET on the Debye length λ_D. The reported biomolecule model is constituted by $m = 3$ charges (system charge -1) at constant internal distances. The signal is evaluated at different distances D (in nm) from the nano-wire surface. a) The system is the same as in Fig. 2e and Fig. 2S†c but approaches the surface from the opposite direction. b) The predicted signal.

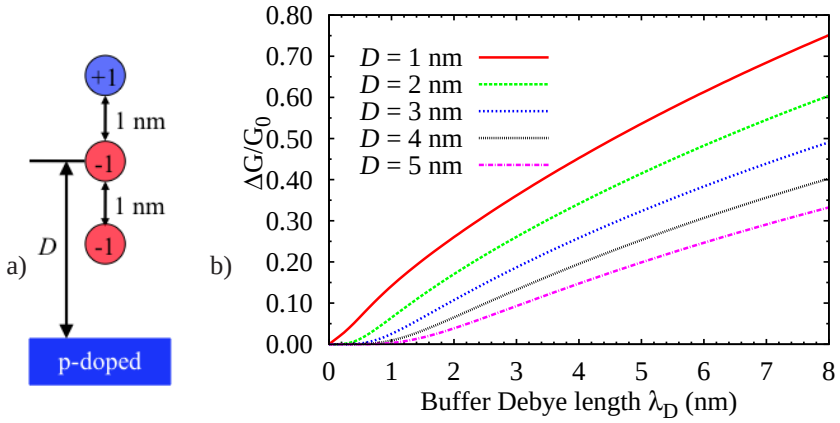

Fig. 7S† Dependence of the conductance sensitivity (signal) of a Si p-type doped nano-BIOFET on the Debye length λ_D. The reported biomolecule model is constituted by $m = 3$ charges (system charge -1) at constant internal distances. a) The system is the same as in Fig. 2e and is anchored to the surface at a distance of 1 nm. (D = 2 nm) b) The same system is tilted by 45° around the anchor point. c) The predicted signals.

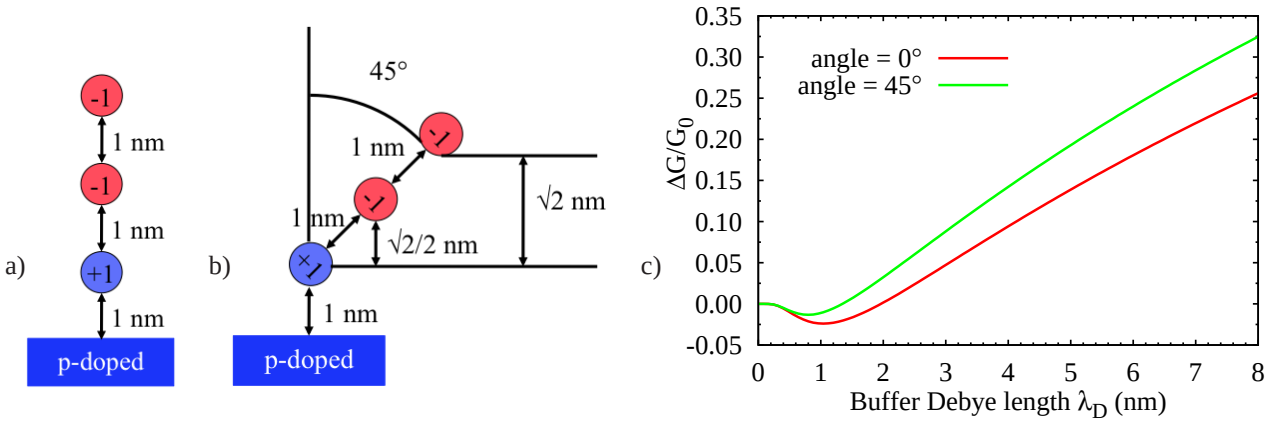

Protein treatment

The crystal structure of each protein, as pdb file, is cleaned of any water molecules and extra residues. In order to ensure that every amino-acid has its proper lateral chain, we use the PDB2PQR program.[12] Using the program VMD[13] we locate the center of mass of each apoprotein, center the protein structure on these coordinates and orient it along its main rotational axis. The minimum and maximum coordinate values along each axes are found, and assumed as the coordinates of the vertices of the rectangular parallelepiped enclosing the protein, which we use as an approximation of the protein itself. We consider the wire surface as completely coated with proteins, that is the ideal situation when the linking of proteins to the wire surface is perfectly efficient. Once the face upon which the protein is residing on the wire surface is defined, by dividing the total wire surface by the area of such face gives the number of residing proteins, and consequently the charge density.

Streptavidin

Tetramer:

Fig. 8S† reports the X-ray structure[14] of the tetrameric form of Streptavidin, with the dimensions of the encompassing parallelepiped. The cavities for the recognition of biotin are on the *yz* face, which has an area of 31.35 nm^2. Supposing full coverage, the surface of the nano-wire described in Table 1S† can accomodate 4727 proteins, while the surface of the nano-wire described in Table 2S† can accomodate 2004 proteins.

Fig. 8S† The structure of the tetrameric form of Streptavidin.

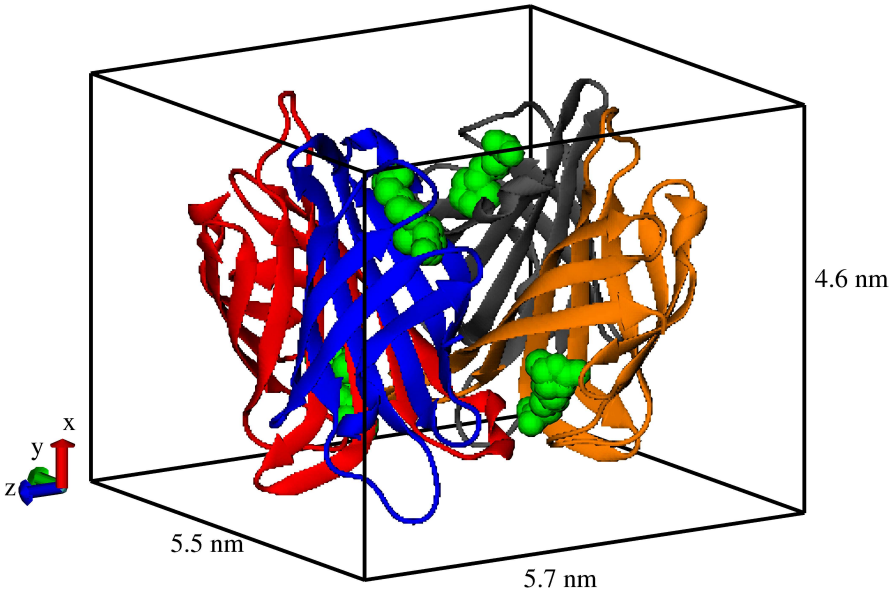

Single chain:

Fig. 9S† reports the X-ray structure[14] of a single chain of Streptavidin, with the dimensions of the encompassing parallelepiped. The cavity for the recognition of biotin is on the *xy* face, which has an area of 10.20 nm^2. Supposing full coverage, the nano-wire surface (Table 2S†) can accomodate 6160 proteins.

Fig. 9S† The structure of a single chain of Streptavidin.

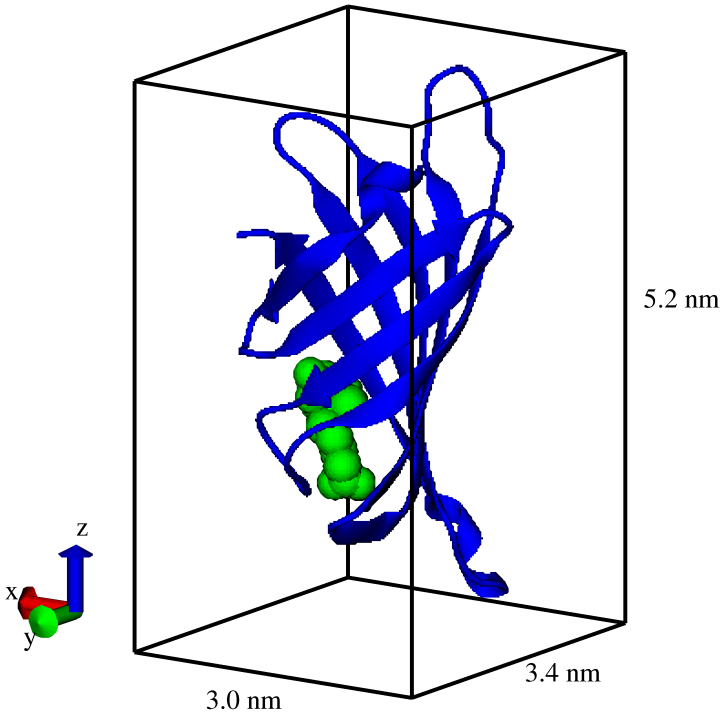

Fig. 10S† Dependence of the conductance sensitivity (signal) of the In_2O_3 n-type semiconducting nano-BIOFET from the Debye length λ_D for the Streptavidin protein (4 interdigitated chains, natural form) at different pH values.

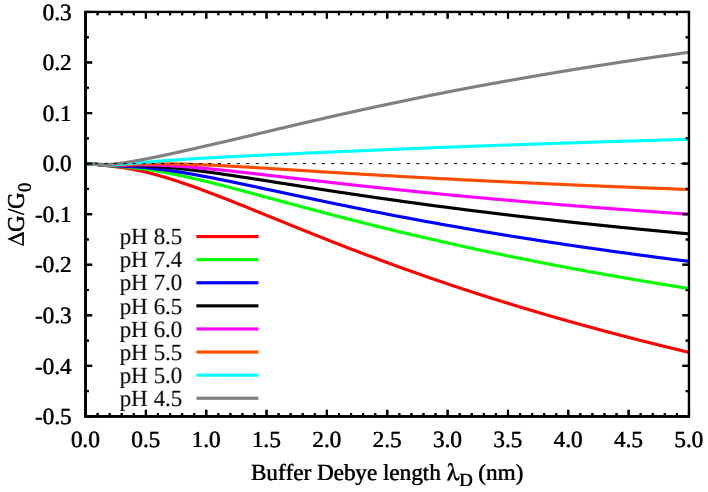

Fig. 11S† Dependence of the conductance sensitivity (signal) of a In_2O_3 n-type semiconducting based nano-BIOFET on the Debye length λ_D for the Streptavidin protein (1 single chain, $N = 6160$) linking to a biotinylated surface. a) Structure of the chain A of the Streptavidin protein (in gray) with the position of the biotin molecule in green. Superimposed, the position of the ionizable amino acids ($m = 26$, system charge -2.18 as computed at pH 7.4) as spheres differently colored, as in Fig. 4. The structure is aligned with the depicted axes. The nano-wire surface is supposed to be 2.65 nm distant from the protein COM (yellow sphere) along the negative direction of the z axis. b) The computed signal.

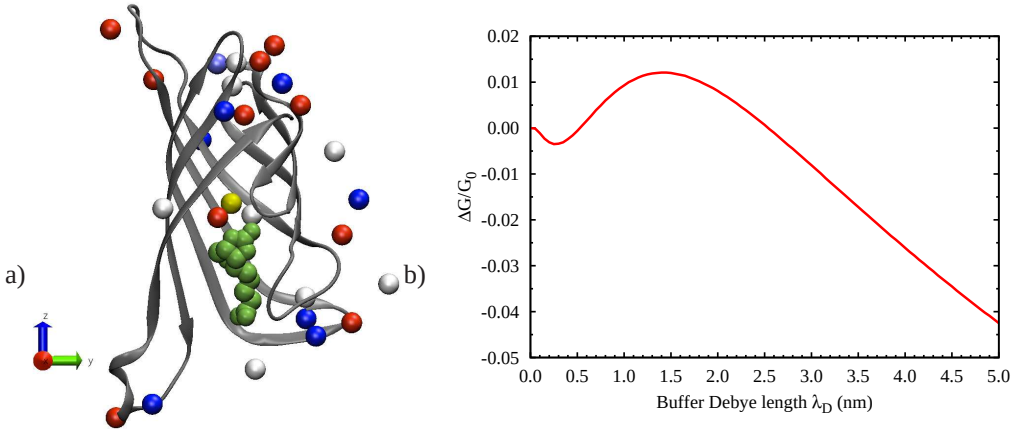

N protein

Fig. 12S† reports the NMR structure[15] of N protein, with the dimensions of the encompassing parallelepiped. In their experiments, Ishikawa et al.[11] functionalize their nano-wires with engineered Fibronectin, to which a linker molecule connects the N protein. In their supporting information is reported that the Fibronectin constitutes a layer ca. 4.3 nm thick. Fig. 13S† reports the structure of the linker molecule structure after a simple energy minimization, and the distance between the Fibronectin anchor atom (P) and the anchor for the N protein (S). Overall, the bio-functionalization layer can be thought as ca. 6 nm thick. See Ref. 11 for further details on the bio-functionalization layer.

Depending on the direction of approach to the nano-wire surface (Table 2S†) and supposing full coverage, a different number of proteins can be accomodated on the surface, as reported in Table 3S†.

Fig. 12S† The structure of N protein.

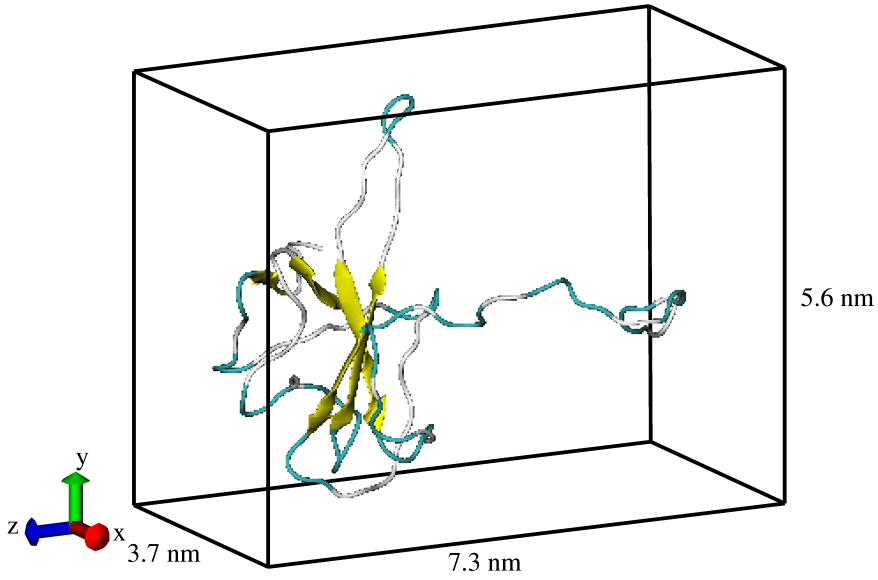

Fig. 13S† Linker molecule structure.

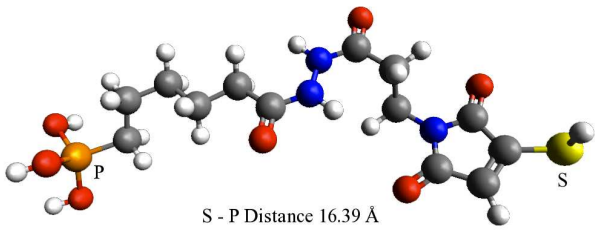

Table 3S† N protein COM - nano-wire surface distance, when the protein approaches from different directions. For each distance, 6 nm for the bio-functionalization layer are included. By changing the approaching direction, the number of proteins N considered for full coverage changes accordingly.

Direction	Distance (nm)	N	Direction	Distance (nm)	N	Direction	Distance (nm)	N
$+x$	7.8	3381	$+y$	9.3	5118	$+z$	8.6	6671
$-x$	7.9	3381	$-y$	8.3	5118	$-z$	//	//

Notes and References

1 M. H. Sørensen, N. A. Mortensen and M. Brandbyge, *Appl. Phys. Lett.*, 2007, **91**, 102105.
2 M. H. Sørensen, *Nanowires for chemical sensing in a liquid environment*, 2007, Bachelor Thesis.
3 F. W. J. Olver, in *Handbook of Mathematical Functions with Formulas, Graphs, and Mathematical Tables*, ed. M. Abramowitz and I. A. Stegun, Dover, 1973, pp. 355 – 436.
4 Y. Cui, Z. Zhong, D. Wang, W. U. Wang and C. M. Lieber, *Nano Lett.*, 2003, **3**, 149–152.
5 B. G. Yacobi, *Semiconductors Materials An Introduction to Basic Principles*, Kluver Academic Publisher, New York, 2003, p. 54.
6 L. De Vico, M. H. Sørensen, L. Iversen, D. M. Rogers, B. S. Sørensen, M. Brandbyge, J. Nygård, K. L. Martinez and J. H. Jensen, *Nanoscale*, 2011, **3**, 706–717.
7 I. Hamberg and C. G. Granqvist, *J. Appl. Phys.*, 1986, **60**, R123–R160.
8 J. R. Bellingham, W. A. Phillips and C. J. Adkins, *J. Phys.: Condens. Matter*, 1990, **2**, 6207–6221.
9 C. Li, D. Zhang, S. Han, X. Liu, T. Tang, B. Lei, Z. Liu and C. Zhou, *Ann. N.Y. Acad. Sci.*, 2003, **1006**, 104–121.
10 H. Köstlin, R. Jost and W. Lems, *Phys. Status Solidi A*, 1975, **29**, 87–93.
11 F. N. Ishikawa, H.-K. Chang, M. Curreli, H.-I. Liao, C. A. Olson, P.-C. Chen, R. Zhang, R. W. Roberts, R. Sun, R. J. Cote, M. E. Thompson and C. Zhou, *ACS Nano*, 2009, **3**, 1219–1224.
12 T. J. Dolinsky, J. E. Nielsen, J. A. McCammon and N. A. Baker, *Nucleic Acids Res.*, 2004, **32**, W665–667.
13 W. Humphrey, A. Dalke and K. Schulten, *J. Mol. Graphics*, 1996, **14**, 33–38.
14 P. Weber, D. Ohlendorf, J. Wendoloski and F. Salemme, *Science*, 1989, **243**, 85–88.
15 Q. Huang, L. Yu, A. Petros, Andrew M.and Gunasekera, Z. Liu, N. Xu, P. Hajduk, J. Mack, S. W. Fesik and E. T. Olejniczak, *Biochemistry-US*, 2004, **43**, 6059–6063.